Adaptive Speckle Reducing Anisotropic Diffusion Filter for Positron Emission Tomography Images Based on Anatomical Prior

Mousa Alrefaya[1,2]
Dept. of Information Technology[1]
Palestine Polytechnic University
B.O Box 198, Herbon, Palestine.
mousa@ppu.edu

Dept. of Electronics and Informatics - ETRO-IRIS[2]
Vrije Universiteit Brussel
Pleinlaan 2
B-1050 Brussels, Belgium

***Abstract*— Positron Emission Tomography (PET)/Computed Tomography (CT) is the main medical imaging technique which used for diagnosing cancer. PET image is showing the functional activities in the patient while CT imaging presents the anatomical information. The PET raw-projection data (sinogram) contains a very high level of Poisson noise, while The reconstructed image through filtered back-projection algorithm (FBP) is contaminated with unknown noise that is very similar to speckle noise distribution. This noise may lead to increase the doze of radioactive material that given to the patient for imaging PET and to errors in the diagnosis results. Applying a suitable filtering approach can increase the effectiveness of the diagnosing process. Using the high resolution information in the CT, we propose in this work an adaptive post-reconstruction curvature motion filtering technique for PET image. The proposed filter consider computing the diffusivity function (edge stopping function) based on the fused image (PET/CT) to guide the smoothing and the sharpening process in the image. Experiments demonstrate through simulated images that the performance of the proposed method significantly enhance the reconstructed PET using FBP algorithm. Further, it compared with recently published methods, both visually and in terms of statistical measures.**

Keywords - SRAD; Positron emission tomography; Nonlinear diffusion; PET enhancement; Shock filter

I. INTRODUCTION

Positron emission tomography allows the imaging of functional properties of the living tissue, whereas other modalities (CT, MRI) provide structural information at significantly higher spatial resolution compared to PET. In the PET imaging, introducing anatomical prior constraint for enhancing PET images during reconstruction or post-reconstruction is proved to improve significantly the quality of the results [21], [1].

Finding a suitable denoising method for enhancing PET still consider as a hot topic for researcher in the medical image processing area. Filtering methods based on PDE schemes have been proved to be effective in reducing the noise and keep important features if the noise characteristics is well identified and a suitable edge stopping function is used.

In our previous work [31], [29], we have proposed a Probabilistic Curvature Motion pre-reconstitution filter for enhancing the PET image by filtering the PET raw data (sinogram) and the results were very promise. The proposed method was initiated based on the curvature motion filter, the probabilistic edgge stopping function, and considering that the noise in the sinogram is a priori identified as a Poisson noise.

The noise distribution in reconstructed PET images that created by FBP is very well characterized by gamma distribution followed closely by normal distribution, based on the study of Teymurazyan, et. al. [4]. Image noise, is in this work, described by an Speckle noise which follows a Gamma distribution and an additive noise model. Based on the anisotropic diffusion and Gamma distribution a new model for speckle reduction is developed. It called as speckle reducing anisotropic diffusion (SRAD) method. SRAD is very suitable for speckle reducing which enhances PET image, as well preserves and enhances edges.

Recently, there has been a considerable interest in cooperating the structural information derived from anatomical image such as MRI or CT to enhance the signal-to-noise ration of the reconstructed PET. In this work, a novel anatomical based anisotropic diffusion for PET image is introduced.

This paper is organized as follows. Section 2 illustrate the literature review of this topic.The theoretical background and terminology used through this paper is introduced in section 3. The proposed method is presented in section 4. Section 5 describes the experimental framework used to evaluate the performance of the proposed algorithms and discussed the results. Our conclusion is presented in section 6.

II. LITERATURE REVIEW

Recently, many researcher have been working on developing PET image enhancing methods with and without anatomical prior. In this section, recent works are presented and discussed.

In the study of Chan et al. [9], a non-local means (NLM) post-filtering algorithm for PET images with incorporating anatomical knowledge from co-registered computed tomography CT image was proposed and denoted adaptive non-local means (A-NLM). The NLM estimates the denoised pixel $NL(x_i)$ as the mean of the intensity values of all pixels whose Gaussian neighborhood resembles the neighborhood of x_i within the image X. The NLM method is formulated as: $NL(x_i) = \sum_{j \in N(i)} w_{ij} x_j$

where w_{ij} is the weight that measures the similarity of the vectors x_i and x_j, $w_{ij} \in [0, 1]$ and $\sum_j w_{ij} = 1$; these vectors denote a square neighbourhood of fixed size, centered at pixels x_i and x_j. $N(i)$ denotes the search window centered at the current pixel x_i. The similarity is measured by a function of the Gaussian-weighted Euclidean distance between x_i and x_j.

A simulated PET emission scan of a digital phantom resembling the human thorax was used for evaluating Chan et al. method. The total number of counts in the sinogram was 950,000 and 50 noise realizations with Poisson noise added. The quantitative evaluation was made using lesion to background contrast curve. The results demonstrate that A-NLM yields better performance in suppressing noise compared with conventional Gaussian post-filtering and NLM.

Another approaches for incorporating anatomical prior information into filtering PET images during reconstruction was proposed in [8], [5]. Authors in [8] proposed an anatomically based Anisotropic Median-Diffusion Filtering during reconstruction. In [5], Chan et al. proposed another approach based on using the anatomical information in two separate ways: the anatomical boundary definition was used to influence the estimation of emission values in proximity to the boundaries in the PET image, while the organ region information was used to estimate an anatomically adaptive anisotropic median-diffusion filter to generate a smoothing prior for the next iteration in the reconstruction process. The Perona and Malik diffusion function was adopted in [5], $\frac{\partial u}{\partial t} = u_t = div(g(|\nabla u|)\nabla u) \qquad u(0) = u_0$ where u is the smoothed image, u_t is the partial derivative of u with respect to diffusion time t, 'div' denotes the divergence operator and $g(|\nabla u|)$ is the so-called edge stopping or diffusivity function, given as: $g(|\nabla u|) = \frac{1}{1+\frac{|\nabla u|^2}{K^2}}$ where K is the contrast parameter and $|\nabla u|$ is the image gradient.

Authors evaluated the proposed method by applying it to a computer-simulated disc phantom, a simulated digital phantom resembling the human thorax and a physical torso phantom. Quantitative evaluations of the 100 noise realizations were made using lesion to background contrast and normalized root mean square error.

In another recent study of Chan, el al. [20] a post-reconstruction nonlocal means (NLM) filter is applied of the PET imaging by combining anatomical information from a CT. This filtering algorithm smoothing the noise by computing the weighted average of voxels based on measuring the similarity between patches of voxels within the image. Anatomical knowledge obtained from CT was incorporated to constrain the similarity measurement within a subset of voxels. The proposed method was compared to Gaussian, edge-preserving bilateral and the median nonlocal means (MNLM) filtering without an anatomical prior.

A non-local means (NLM) post-reconstruction filtering for SPECT is proposed is [27]. Authors investigated using NLM filtering as a post-reconstruction filtering method, with and without CT side information, to enhance SPECT imaging. Phantom with tumors containing a uniform and a non uniform activity distribution were applied for the evaluation. Using CT information for filtering SPECT is found to give better enhanced images and robust to small misregistration between SPECT and CT information. Based on measuring the contrast recovery they concluded that using more OSEM iterations is essential for accurate estimation. The results is compared with conventional Gaussian filtering and to unfiltered methods.

Kennedy et al. [11], proposed a postprocessing algorithm for incorporating anatomical edge from CT with functional PET data to improve the PET image quality. The anatomical information from CT and the PET texture data were merged using a modified Hybrid Computed Tomography algorithm (HCT). In the combined PET/CT images, each PET pixel value was estimated by iteratively applying a corrected 2D Taylor expansion to each of its eight neighbors. In other words, the CT edges are considered rather than the PET edges.

The proposed algorithm was tested on a special resolution phantom and patient data sets. The Contrast ratios was applied for testing the method.

An algorithm for enhancing the blurred PET images, using registered Computed Tomography (CT), is proposed in [24]. The algorithm is based on a forward-and-backward anisotropic diffusion. A forward diffusion is utilized to stabilize the process. The proposed method is tested with real measured PET/CT data. The proposed method is implemented and tested on 3D data. The anatomical information (CT) is introduced for sharpening the PET image edges by deneing the diffusion tensor based on CT gradients. PET intensity flows through CT gradients, creating PET edges along the CT ones. The analysis for combining CT for enhancing PET shows four primary cases:
(1) High PET and high CT gradient magnitudes. In this case, PET edges are strong along CT ones, so no further sharpen is needed and both processes should slow down.
(2) Low PET gradient magnitude with high CT gradient magnitude. Here, more sharpening is required to enhance edges, so the backward force should be emphasized.
(3) High PET gradient magnitude with low CT gradient magnitude. This occurs when PET edges are falsely created where no tissue boundary is present. This may be due to over-sharpening, or reconstruction noise. In this case, the forward process should have greater emphasis.
(4) Low PET gradient magnitude with low CT gradient magnitude. Here, the process should not affect the image, as these conditions are present within tissues in normal case.

A wavelet synergistic approach that combines functional and structural information (e.g. CT/MRI) for enhancing PET images is proposed and studied in [10], [23]. In this method, the PET image and the anatomical CT/MRI image are decomposed into several resolution elements. Then, the PET high-resolution elements are replaced with those of the CT/MRI image after appropriate scaling.

Filtering approach based on fuzzy nonlinear anisotropic diffusion with non-local means is proposed in [7] to improve the quality of PET images. The proposed method combined the Penalized Maximum likelihood algorithm with nonlocal fuzzy anisotropic diffusion to adapt the diffusion coefficients according to the characteristics of the reconstructed image. Since,the diffusion processing can be considered as fuzzy classification as more pixels belong to the smooth region, stronger diffusion will apply. The diffusion coefficient is represented by a membership function.

Results showed that the new approachs better in suppressing noise and preserving edges.

Filtering SPECT image by a non-local means (NLM) method with and without CT information is studied in [25]. Two ways to incorporate CT side information during reconstruction in the adopted ltering approach is investigated. Simulation results with two uniform tumors showed that the proposed ltering method with anatomical information decreased the error as compared. In another study, a nonlocal regularization method for PET image reconstruction with an anatomical images is proposed in [26]. The proposed method applied to anatomy-based PET image reconstruction. Results showed enhanced image resolution compared to the conventional method based on local smoothing as well as the reconstruction accuracy even with the imperfect prior anatomical information.

In another study [21], a new approach is proposed for measuring the similarity between functional and anatomical image to incorporate the anatomical information for better enhancing the PET images based on the joint entropy approach. The new approach take into account dependence of the two images on the underlying tissue composition.

Using three different MRI anatomical priors for improving PET brain imaging are studied in [22]. The investigated methods for combining the prior are: i) a prior based on a segmentation of the MRI image; ii) the joint entropy prior and iii) a Bowsher prior. $neighborhood, computed from the MRI image.$

Results showed that the Bowsher prior performance is better than other priors.

III. Theoretical Background

In this section we present some of the related studies to the proposed method and the theories behind these studies.
In [17], Bettahar et al. proposed a PDE-based filter which combines shock filter and curvature diffusion. This model removes noise and sharpens edges. Additionally, it preserves well the location of the shocks by synchronizing both effects of smoothing and deblurring. Lets first introduce the theory behind the shock filter.

A. Shock Filter

The 2D formulation of the classical shock filter with reflecting boundary conditions is commonly given by [16]:

$$u_t = -sign(G_\sigma * u_{ww})u_w \tag{1}$$

where u_t is the image solution at time t and $u(0) = u_0$ is the input image. w is the direction of the gradient ∇u with:

$$\begin{aligned} u_{ww} &= \frac{u_{xx}u_x^2 + 2u_x u_y u_{xy} + u_{yy}u_y^2}{\left(u_x^2 + u_y^2\right)} \\ u_w &= |\nabla u| = \sqrt{u_y^2 + u_x^2} \end{aligned} \tag{2}$$

The convolution of u_{ww} with the Gaussian function $G\sigma$, where σ is the standard deviation of the Gaussian, is used to make the filter more robust against noise. The main idea of the shock filter assumes that some pixel is in the influence zone of a maximum, where its second derivative u_{ww} is negative. Then (Equ. 2) becomes: $u_t = |\nabla u|$

Evolution under this PDE is known to produce at time t a dilation process with a disk-shaped structuring element of radius t. At the influence zone of a minimum with $u_{ww} > 0$, Equ. (2) can be reduced to an erosion equation with a disk-shaped structuring element: $u_t = -|\nabla u|$

These considerations show that for increasing time, the radius of the structuring element is increased until it reaches a zero-crossing of u_{ww}, where the influence zones of a maximum and a minimum meet. Therefore, the zero-crossings of the derivative u_{ww} serve as an edge detector, where a shock is produced that separates adjacent segments.

B. Bettahar's Image Filtering Model

The Bettahar's [17] image filtering model is given as:

$$\begin{aligned} u_{t+1} &= |\nabla u| \text{div}\left[g_1(|\nabla u|)\frac{\nabla u}{|\nabla u|}\right] - P_\alpha |\nabla g_2(|\nabla u|)|^2 (u_t - \xi_t) \\ \xi_t &= P_\beta (1 - |\nabla g_2(|\nabla u|)|^2) u_{ww} - sign(G_\sigma * u_{ww})|\nabla u| \end{aligned} \tag{3}$$

The functions $g_1(|\nabla u|)$ and $g_2(|\nabla u|)$, in Equ. 3, were given as:4

$$\begin{aligned} g_1(|\nabla u|) &= \frac{1}{1+|\nabla u|^2/k_1^2} \\ g_2(|\nabla u|) &= \frac{1}{1+|\nabla u|^2/k_2^2} \end{aligned} \tag{4}$$

The first function $g_1(|\nabla u|)$ is used to assure an anisotropic behavior, and to select small edges to be smoothed according to the parameter k_1 while $g_2(|\nabla u|)$ is introduced to select which strong edges to be improved according to k_2. The parameters P_α and P_β are positive balance constants. The first part of the first equation in 3 is the curvature diffusion process, where the second one is a shock filter coupled to a kind of diffusion. The second equation diffuses the image only in the direction of the gradient, especially at isolated artificial edges, which can be created by noise. This equation is used to remove noise at noisy edges and to create a shock in these locations, where $|\nabla g_2(|\nabla u|)|$ tends to zero.

C. Speckle Reducing Anisotropic Diffusion

The characteristic of the noise in PET images created by FBP is very well characterized by gamma distribution followed closely by normal distribution, based on the study of Teymurazyan, et. al. [4]. Image noise, is in this work, described by an Speckle noise which follows a Gamma distribution and an additive noise model, as follows:

$$f = eI + n \tag{5}$$

where f is the observed noisy image, I is the true image, e is the noise which follows a Gamma Law with mean one (in this study e is considered a Speckle noise as it follows a gamma distribution [18]) and n is the additive Gaussian noise. Speckle noise is one of the most complex image noise models. It is signal independent, non-Gaussian, and spatially dependent.

Based on the anisotropic diffusion and Gamma distribution a new model for speckle reduction is developed [19], [13], [12]. It called as speckle reducing anisotropic diffusion (SRAD) method. SRAD is very fit for speckle reducing which preserves and enhances edges. Given an intensity image $u_0(x, y)$, the output image $u(x, y, t)$ is evolved according to the following PDE:

$$\frac{\partial u(x, y, t)}{\partial t} = div(c(q)\nabla u(x, y, t)) \tag{6}$$

Where $u(x, y, 0) = u_0(x, y)$ and t represents diffusion time, $c(q)$ is given as:

$$c(q) = \frac{1}{1 + [q^2(x, y, t) - q_0^2(t)]/[q_0^2(t)(1 + q_0^2(t))]} \tag{7}$$

Where $q(x,y,t)$ is the instantaneous coefficient of variation determined by

$$q(x,y,t)=\frac{(1/2)(|\nabla u|/u)^2-(1/4^2)(\nabla^2 u/u)^2}{[1+(1/4)(\nabla^2 u/u)]^2} \tag{8}$$

And q_0 is the scale factor of speckle, can be estimated as [19]: $q_0(t)=\frac{\sqrt{var[E(t)]}}{E(t)}$ Where var $[E(t)]$ and $E(t)$ are the intensity variance and mean over a homogenous area at t, respectively.

The above mentioned function, q which is the instantaneous coefficient of variation $q(x,y,t)$ helps in detecting the edges present in the images corrupted by speckle. At edges and high contrast regions this function produces high values and at homogeneous regions it gives low values, $q_0(t)$ is the speckle scale function and $q(x,y,t)$ fluctuates around $q_o(t)$.

IV. The proposed method: ASRAD for PET

In order to improve the important features in the PET images (i.e tumors) and considering [13], [12], [4], [17], [7] and Chan's studies [5], [9], we propose a novel adaptive SRAD non-linear curvature diffusion-shock filer with anatomical prior. In our case, this enhances smoothing homogeneous regions via constraint curvature motion via the function $c(q)$ (Equ. 7) here q is estimated locally, as given in [19]. Further, the proposed method combine anatomical information from aligned CT images for enhancing significant information in the PET image.

The anatomical information are used for weighting the sharpening process. The edge stopping function is obtained based on a combined PET/CT image and is used for controlling the sharpening term. In the following, we introduce the proposed scheme.

Let f and z denote accurately aligned PET and CT images respectively. The proposed scheme is given as:

$$\begin{aligned}
&u_{t+1}=c(q)(u_{vv}+u_{ww})+\alpha|\nabla g_2(|\nabla F|)|^2(u_t-\xi)\\
&\xi=P_\beta(1-|\nabla g_2(|\nabla F|)|^2)u_{ww}-sign(G_\sigma * F_{ww})_t|\nabla F_t|\\
&F_t(i,j)=a.u_t(i,j)+b.z(i,j)\\
&u_{t=0}=f(.)\\
&u_n=0
\end{aligned} \tag{9}$$

u_t is denoted the scale-space image, and the scale $t\in\mathcal{R}^+$. The enhanced version of the observed noisy PET,f, is a given u_t that yields an estimate of the unknown noise-free version of f. The Von-Neumann boundary condition on the boundary, n, of the image domain is adopted. ξ represents the regularized recontracted PET.

The parameters α and β are balance constants, u_{vv} is the second order Gauge derivative of the image along the image edges, and the third term is the shock filter based on the combined (fused) PET/CT image. where the Weighted Averaging algorithm is adopted for combining PET/CT images. F is the fused image, a and b represent the weighting factors for the both images. The Weighted Averaging method is easy to implement and fast to execute. We propose to set a=0.7 and b=0.3.

in this work, I will test the following diffusion controlling functions q:

1- $c(q)_{PET}$ formula based on the PET image, where q is given as:

$$q(x,y,t)=\frac{(1/2)(|\nabla u|/u)^2-(1/4^2)(\nabla^2 u/u)^2}{[1+(1/4)(\nabla^2 u/u)]^2} \tag{10}$$

2- $c(q)_{CT}$ formula based on the CT image, where q is given as:

$$q(x,y,t)=\frac{(1/2)(|\nabla z|/z)^2-(1/4^2)(\nabla^2 z/z)^2}{[1+(1/4)(\nabla^2 z/z)]^2} \tag{11}$$

3- $c(q)_{Fused}$ formula based on the fused PET-CT image, where q is given as:

$$q(x,y,t)=\frac{(1/2)(|\nabla F|/F)^2-(1/4^2)(\nabla^2 F/F)^2}{[1+(1/4)(\nabla^2 F/F)]^2} \tag{12}$$

where z is the anatomical image, F is the fuzed PET-CT image.
and g_2 are of the form:

$$g_2(|\nabla z|,k)=\frac{1}{1+\frac{|\nabla z(i,j)|^2}{k^2(i,j)}} \tag{13}$$

where k is a contrast free parameter which is estimated locally. The co-registered CT image is degraded to the resolution of the PET image. This can be done by applying the CT volume an isotropic gaussian kernel so that final image resolution matched the one of the PET scanner.

We adopt Samsonov's method [15] for the edge stopping functions $g_2(|\nabla u|k)$. As we present in section III, this method is locally-based where parameter k is dependent on the local noise properties and computed at each location (i,j) in the image.

For images with varying noise levels, by using this method we avoid the CT segmenting problem that was used for modifying the k parameter as proposed in Chan's works [5], [9].

Description of the proposed model:

Term 1 $[c(q)(|\nabla u|).u_{vv}]$
The first part of the proposed filter is the SRAD non-linear curvature diffusion. This diffuses the image only in the direction of the level set. This equation is used to remove Spekele noise as much as possible. u_{vv} is given as:

$$u_{vv}=|\nabla u|div\left(\frac{\nabla u}{|\nabla u|}\right)=\frac{u_{xx}u_y^2-2u_xu_yu_{xy}+u_{yy}u_x^2}{\left(u_x^2+u_y^2\right)} \tag{14}$$

The above mentioned function, q which is the instantaneous coefficient of variation $q(x,y,t)$ helps in detecting the edges present in the images corrupted by speckle. At edges and high contrast regions this function produces high values and at homogenous regions it gives low values, $q_0(t)$ is the speckle scale function.

Term 2 $[\alpha|\nabla g_2(|\nabla F|,k)|^2(u_t-\xi)]$
On the other hand, the second part is an anatomical-based sharpening term. The parameter α is used for balancing the weight of this term and is selected empirically. The anatomical information is used and combined in implicit way for controlling and improving the filtering results of the PET images. The anatomical information from CT is used for weighting the enhancing term in the proposed filter via ξ and for guiding the enhancing and the sharpening process via g_2. The first derivative of g_2 ($\nabla g_2(|\nabla F|,k_2)$) in the second term make backward diffusion possible. This give the filter the capability of edge enhancement and improve the edges in the PET image according to the combined edges in the (PET/CT) fused image. The fused image is computed at each iteration for. The edges will be sharpened by the weighed difference between u_t and ξ.

Unlike the method of Turkheimer, et al. [10] where the anatomical information and edges are explicitly inserted and merged in the PET image which may create new unwanted patterns, our method avoids creating new patterns or edges in the PET image. As this may cause a false positive diagnosis result.

Why using fused image?
PET and CT images provide different views of the body (functional and anatomical). For this reason, we propose to combine the anatomical and functional information in one image and then to obtain the edge stopping function g_2 based on the gradient of the combined image. In the fusion process, we increase the weights of PET and reduce the CT ones to reduce the effects of the unimportant information from the CT. The adopted method which is frequently used in the literature for image fusion [14]is the Weighted Averaging:

At transition locations $|\nabla g_2(|\nabla F|,k_2)|$ is high of the equation will be active and will operate like a sharpening term. Through using fused image F and first derivative of the edge stopping function $g_2(|\nabla F|,k)$, the sharpening term are carefully controlled for enhancing the weak and vanish edges.

Term 3 $[\beta|sign(G_\sigma * F_{ww})|\nabla F|]$
The third term in this filter is a shock filter that enhance the weak edges and creates a shock in these locations, especially at isolated artificial edges, which can be created by noise. The parameter β is used as a balance between diffusion and shock effects. This term is based on the PET/CT fused image to enforce edges from the CT image for enhancing weak edges in the PET. The zero-crossings of the derivative F_{ww} serve as an edge detector in the fused PET/CT image, where a shock is produced that separates adjacent segments.

V. Experiments and Discussion

For the analysis of the proposed denoising approaches, we use a simulated thorax PET phantom, containing three hot regions of interest (tumors) (1.18, 1.8 and 1.57) was constructed. 50 realizations (noisy sinograms) with added noise of $1\text{x}10^6$ coincident events, have been generated. Each sinogram has a size of $256\text{x}256$ pixels and their spacing is $2\text{x}2\frac{\text{mm}}{\text{pixel}}$, with 128 detectors and 128 projection angles. Figure.4(a) shows the ideal noise-free sinogram with the PET images obtained via the FBP (Fig.4(d)) reconstruction. A corresponding noise contaminated realization is shown in Fig.4(b),(e)-(f). The quantitative accuracy of PET images is degraded by the limited spatial resolution of the CT. For the purpose of degradation in resolution, the point-spread function (PSF) tends to be approximated by an isotropic Gaussian.

A. *Quantitative Evaluation Measures*

Two types of evaluation measures are adopted [31], [29]. The first set based on measuring the quality of the filtering techniques whilst the second set originates from validating the quality of the PET reconstruction. As ground-truth information, the first type uses the noise-free image, whilst the second type needs prior identification of the important areas by a radiologist.

Denoising Quality: (DQ) The idea is to verify the quality of the denoised sinogram, u_t, with respect to the noise-free image I. In this work, we adopt the following measures [30]: DQ1

1) The Peak Signal to Noise Ratio (**PSNR**) is a statistical measure of error, used to determine the quality of the filtered images. It represents the ratio of a signal power to the noise power corrupting, so the higher the PSNR, the better the quality.

$$PSNR(t)=10\log_{10}\frac{\text{Card}(\Omega)}{\sum_{p\in\Omega}|I(p)-u_t(p)|} \tag{15}$$

2) The correlation ($\mathcal{C}_{\mathbf{m}\rho}$) between the noise-free and the filtered image. The higher this correlation the better the quality is.

$$\mathcal{C}_{m\rho}(t) = \rho\left[I, u_t\right] \tag{16}$$

3) The calculated variance of the noise (***NV***) describes the remaining noise-level. Therefore, it should be as small as possible.

$$\mathrm{NV}(t) = Var\left(|I - u_t|\right) \tag{17}$$

In this work, we are interested in comparing the maximum of each measure for different filtering approaches.

For PET filtering application, we use an earlier proposed optimal scale selection approach [30], where the maximum correlation method has been adopted:

$$t_{opt} = \operatorname{argmax}\left[\widehat{\mathcal{C}}_{mp}(t)\right] = \operatorname{argmax}\left[\sigma[u_t] + \frac{\sigma[n_o(t_0)]}{\sigma[u_{t_0}]}\sigma[n_o(t)]\right] \tag{18}$$

with n_o is the so-called outlier noise estimated using wavelet-based noise estimation. t_0 is the zeroth scale, thus $u_{t_0} = f$ and $n(t_0)$ represents the initial amount of noise.

B. Denoising Quality Results

In this work, we are interested in comparing the proposed filter, namely, the Anatomical-based Adaptive SRAD filter $(SB-ASRAD)_F$ where the function $c(q)$ is build based on the fused image, with $(SB-ASRAD)_{CT}$ where the function $c(q)$ is build based on the anatomical image and with the $(SRAD)$ where the function $c(q)$ is build based on the PET image. Additionally, Perona and Malik filter (P-M) [3] is applied and tested. The Lorentzian diffusivity function $g(X) = 1/(1 + X^2/k^2)$ is used for applying the $P - M$ filters. The free parameters (alpha and beta) and the parameters for the image fusing (a,b) in the proposed filter are manually set.

Figure 2 illustrates the optimal enhanced scale of the filtered reconstructed PET for all considered filtering methods.

The variance image for the filtered PET images are presented in Figure **??**. As it can be seen visual inspections do not allow comparing effectively the different methods. For the qualitative assessment, we calculated the denoising quality measures defined in Section V-A for each filtering schemes. The results are displayed in Table I.

in this paper is remarkable in discriminating the ROI from image noise (see Figure 2). Also notice the improved performance of the $(AB - ASRAD)_F$ algorithm as compared with the performance of the standard diffusion algorithms.

VI. CONCLUSIONS

Anatomical-based Adaptive SRAD filter for enhancing PET images is developed and discussed in this work. The developed filter is applied on the 2D PET post-reconstruction via FBP. It considered the PET noise distribution (the speckle noise) in the filtering process. Anatomical prior (i.e computed tomography) image is combined in building the diffusivity function. The anatomical information are used for weighting the sharpening process. The edge stopping function is obtained based on a combined PET/CT image. The SRAD filter approved to be an effective filter for PET image with speckle noise. The results show that involving anatomical prior in the filtering process improving the quality of the enhanced PET images. This improvement is due to the better resolution of the CT image which leads to better preserving of the significant features. Ab-ASRAD achieved more effectiveness in smoothing all the homogeneous regions that contain high level of noise among other methods and wisely smoothes the region of interest as well as the other regions in the PET image. The contrast recovered better in the ROIs by the inserting the anatomical image in the diffusivity function and introducing the enhancing term in the filter. These filters gives a well smoothed image and preserves the edges, and gains the advantage of the curvature motion diffusion and the shock filter. Further, they deal better with the problem of the poor and discontinuity of edges which is common in the PET images. The proposed algorithm considers all possible cases for combining the anatomical information in the filtering process. Since the edges in the CT images are not completely the same as in the PET image, this algorithm use smart way to insert the anatomical information through the fused PET/CT image via the three filtering terms. Enhancing the weak edges in PET resulted in better diagnosis accuracy for the tumor size and shape.

REFERENCES

[1] A. Mehranian, M. Belzunce, F. Niccolini, M. Politis, C. Prieto, F. Turkheimer, A. Hammers and A. Reader, "PET image reconstruction using multi-parametric anato-functional priors", Physics in Medicine Biology, vol. 62, pp. 5975, 2017.

[2] S. S. Mokri, M. I. Saripan, A. A. Abd Rahni, A. J. Nordin, S. Hashim and M. H. Marhaban, "PET Image Reconstruction Incorporating 3D Mean-Median Sinogram Filtering," in IEEE Transactions on Nuclear Science, vol. 63, no. 1, pp. 157-169, Feb. 2016.

[3] P. Perona and J. Malik, Scale space and edge detection using anisotropic diffusion, IEEE Trans. on Pattern Analysis and Machine Intelligence, vol. 12, pp.629-639, 1990.

[4] A. Teymurazyan, T. Riauka, H.-S. Jans and D. Robinson, "Properties of Noise in Positron Emission Tomography Images Reconstructed with Filtered-Backprojection and Row-Action Maximum Likelihood Algorithm" J. of Digit Imaging., Volume 26, Issue 3, pp 447456, June, 2012.

[5] C. Chan, S. Meikle, R. Fulton, G. J. Tian, W. Cai and D. D. Feng, "A non-local post-filtering algorithm for PET incorporating anatomical knowledge," IEEE Nuclear Science Symposium Conference Record (NSS/MIC), pp. 2728-2732., 2009. doi: 10.1109/NSSMIC.2009.5401971

[6] V. N. Prudhvi Raj, and T. Venkateswarlu, "Denoising of Medical Images Using Image Fusion Techniques", Signal and Image Processing : An International Journal (SIPIJ) Vol.3, No.4, August 2012.

[7] Z. Gui, Y. Liu and J. He, "PML Algorithm for Positron Emission Tomography Combined With Nonlocal Fuzzy Anisotropic Diffusion Filtering," in IEEE Transactions on Nuclear Science, vol. 59, no. 5, pp. 1984-1989, Oct. 2012.

[8] C. Chan, R. Fulton, W. Cai, D. D. Feng and S. Meikle, "Minimum Cross-entropy Reconstruction of PET Images with Anatomically Based Anisotropic Median-Diffusion Filtering," 2007 29th Annual International Conference of the IEEE Engineering in Medicine and Biology Society, Lyon, 2007, pp. 6527-6530.

[9] C. Chan, R. Fulton, D. D. Feng and S. Meikle, "Median non-local means filtering for low SNR image denoising: Application to PET with anatomical knowledge," IEEE Nuclear Science Symposuim Medical Imaging Conference, Knoxville, TN, 2010, pp. 3613-3618.

[10] F.E. Turkheimer, N. Boussion, A.N. Anderson, N. Pavese, P. Piccini and D. Visvikis, "PET image denoising using a synergistic multiresolution analysis of structural (MRI/CT) and functional datasets". J Nucl Med., 49(4):657666, 2008.

[11] J. Kennedy,O. Israel, A. Frenkel, R. Bar-Shalom, and H. Azhari, H., "A hybrid algorithm for PET/CT image merger in hybrid scanners", Eur J Nucl Med Mol Imaging , 34:517-531, 2007.

[12] Y. Zhang and M. Ding, "Low-contrast Edge Enhancing Anisotropic Diffusion for Speckle Reduction," 2010 Fourth International Conference on Genetic and Evolutionary Computing, 2010, pp. 703-708.

[13] K. Krissian, C. F. Westin, R. Kikinis and K. G. Vosburgh, "Oriented Speckle Reducing Anisotropic Diffusion," in IEEE Transactions on Image Processing, vol. 16, no. 5, pp. 1412-1424, May 2007.

[14] B. Yang, Z. Jing and H. Zhao. "Review of pixel-level image fusion". Journal of Shanghai Jiaotong University, Volume 15, No. 1,6-12, 2010.

[15] A. A. Samsonov, and Johnson, "Noise-Adaptive Nonlinear Diffusion Filtering of MR Images With Spatially Varying Noise Levels". Magnetic Resonance in Medicine 52:798806, 2004.

[16] S. Osher, and L.I. Rudin, "Feature-oriented image enhancement using shock filters", SIAM Journal on Numerical Analysis 27 (4), 919940, 1990.

[17] S. Bettahar, and A.B. Stambouli, "Shock filter coupled to curvature diffusion for image denoising and sharpening", Image and Vision Computing, Vol.26,14811489, 2008).

[18] L. Huang, L. Xiao, and Z.-HuiWei "Multiplicative Noise Removal via a Novel Variational Model" Hindawi Publishing Corporation EURASIP Journal on Image and Video Processing Volume 2010, 2010, Article ID 250768.

[19] S. Liu, J. Wei, B. Feng, W. Lu, B. Denby, Q. Fang and J. Dang, "An Anisotropic Diffusion Filter for Reducing Speckle Noise of Ultrasound Images Based on Separability", Signal and Information Processing Association Annual Summit and Conference (APSIPA ASC), pp. 1-4., 2012.

[20] C. Chan, R. Fulton, R. Barnett, D. Dagan Feng and S. Meikle. "Postreconstruction Nonlocal Means Filtering of Whole-Body PET With an Anatomical Prior". TRANSACTIONS ON MEDICAL IMAGING, VOL. 33, NO. 3, 2014.

[21] S. Pedemonte et al., "Class conditional entropic prior for MRI enhanced SPECT reconstruction," IEEE Nuclear Science Symposuim Medical Imaging Conference, Knoxville, TN, 2010, pp. 3292-3300.

[22] A. Atre, K. Vunckx, K. Baete, A. Reilhac and J. Nuyts, "Evaluation of different MRI-based anatomical priors for PET brain imaging," 2009 IEEE Nuclear Science Symposium Conference Record (NSS/MIC), 2009, pp. 2774-2780.

[23] M. Shidahara, C Tsoumpas, C. J. McGinnity, T. Kato, H. Tamura, A. Hammers, H. Watabe and F. E. Turkheimer., "Wavelet-based resolution recovery using an anatomical prior provides quantitative recovery for human population phantom PET [11C]raclopride data", Phys. Med. Biol. 57 (2012) 31073122.

[24] Z. Marta and L. Szirmay-Kalos, "Partial Volume Effect Correction using Anisotropic Backward Diffusion.", Hungarian Association for Image Processing and Pattern Recognition (KEPAF), 2013.

[25] S. Y. Chun, J. A. Fessler and Y. K. Dewaraja, "Non-local means methods using CT side information for I-131 SPECT image reconstruction," 2012 IEEE Nuclear Science Symposium and Medical Imaging Conference Record (NSS/MIC), Anaheim, CA, 2012, pp. 3362-3366.

[26] V. G.Nguyen, and S. G. Lee, " Anatomy-based PET image reconstruction using nonlocal regularization", Proc. SPIE 8313,Physics of Medical Imaging, 2012.

[27] S. Y. Chun, J. A Fessler and Y. K Dewaraja, "Post-reconstruction non-local means ltering methods using CT side information for quantitative SPECT.", Phys. Med. Biol. 58, PP.62256240, 2013.

[28] L. Pogam, H. Hanzouli, M. Hatt, C. Cheze Le Rest and D. Visvikis, "Denoising of PET images by combining wavelets and curvelets for improved preservation of resolution and quantitation", Medical Image Analysis 17(2013), 877891, 2013.

[29] M. Alrefaya and H. Sahli, "A Novel Adaptive Probabilistic Nonlinear Denoising Approach for Enhancing PET Data Sinogram", Journal of Applied Mathematics, Volume 2013, 2013.

[30] I. Vanhamel, C. Mihai, H. Sahli, A. Katartzis, I. Pratikakis, "Scale Selection for Compact Scale-Space Representation of Vector-Valued Images", V International Journal of Computer Vision, Vol. 4485, 2008.

[31] M. Alrefaya and H. Sahli, "Adaptive nonlinear probabilistic filter for Positron Emission Tomography," 2012 IEEE 12th International Conference on Bioinformatics Bioengineering (BIBE), Larnaca, 2012, pp. 703-708.

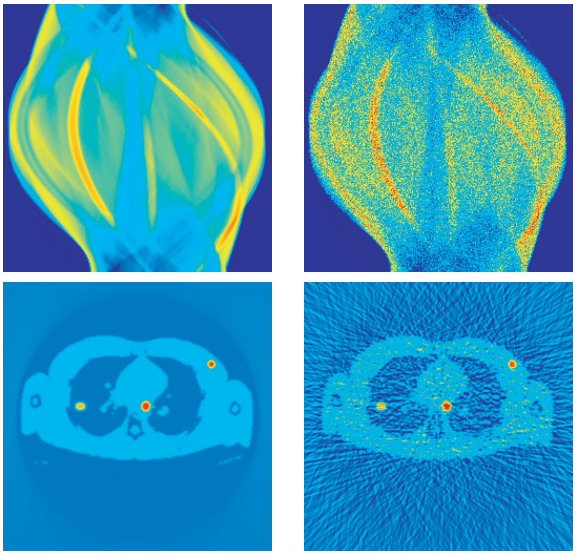

(c) (d)

Fig. 1. (a) The original simulated sinogram and its reconstructed PET image with 3 clearly visible spots: the tumors (ROI) using either FBP reconstruction. (b) An example of one realization noisy sinogram and (c-d) the corresponding reconstructions.

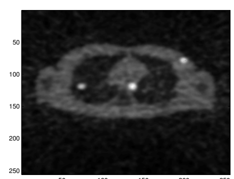

$(a)\ AB - ASRAD_F$

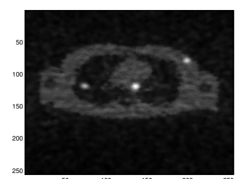

$(b)\ AB - ASRAD_{CT}$

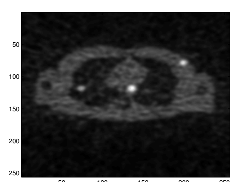

$(c)\ SRAD$

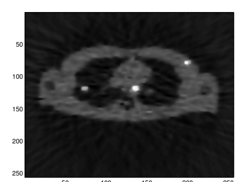

$(d)\ P - M$

Fig. 2. Filtered PET images: figures a and b are examples of the $AB - ASRAD_F$ and $AB - ASRAD_{CT}$ filtering results respectively. The filtering results of the $SRAD$ and $P - M$ are illustrated in figures (c-d) respectively.

TABLE I

DENOISING QUALITY MEASURES

Method	f	AB-ASRAD$_F$	AB-ASRAD$_{CT}$	SRAD	P-M
PSNR(t_{opt})	12.11	24.8	25.1	24.7	21.8
NR(t_{opt})	0.07	0.034	0.032	0.0345	0.024
$C_{m\rho}(t_{opt})$	0.69	0.921	0.992	0.992	0.97

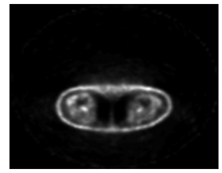

(a:Example of PET real data)

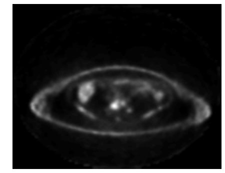

(b:Example of PET real data)

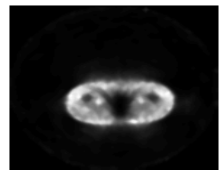

(c: Example: PET for a abdominal)

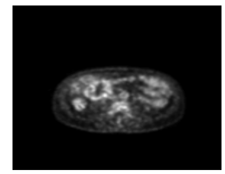

(d: Example: PET for a brain)

Fig. 3. Examples of an experimental real data set

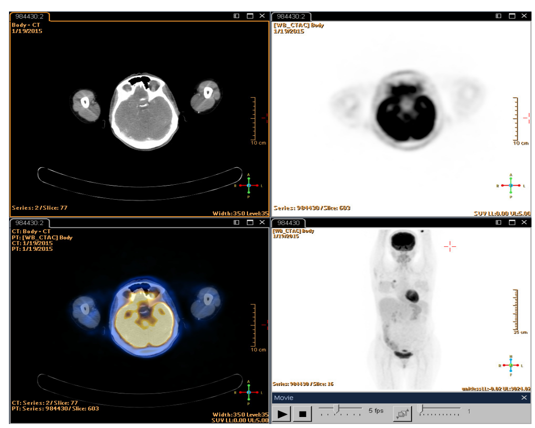

Fig. 4. Examples of a real data set: the upper left image is the CT slice of the brain, the upper right is PET image for the same sector, the lower left is the fused image and the lower right is whole body PET